

RESEARCH

Open Access



Identification of different proteins binding to Na, K-ATPase α 1 in LPS-induced ARDS cell model by proteomic analysis

Xu-Peng Wen¹, Guo Long², Yue-Zhong Zhang³, He Huang⁴, Tao-Hua Liu³ and Qi-Quan Wan^{1*}

Abstract

Background: Acute respiratory distress syndrome (ARDS) is characterized by refractory hypoxemia caused by accumulation of pulmonary fluid, which is related to inflammatory cell infiltration, impaired tight junction of pulmonary epithelium and impaired Na, K-ATPase function, especially Na, K-ATPase α 1 subunit. Up until now, the pathogenic mechanism at the level of protein during lipopolysaccharide- (LPS-) induced ARDS remains unclear.

Methods: Using an unbiased, discovery and quantitative proteomic approach, we discovered the differentially expressed proteins binding to Na, K-ATPase α 1 between LPS-A549 cells and Control-A549 cells. These Na, K-ATPase α 1 interacting proteins were screened by co-immunoprecipitation (Co-IP) technology. Among them, some of the differentially expressed proteins with significant performance were identified and quantified by liquid chromatography-tandem mass spectrometry (LC-MS/MS). Data are available via ProteomeXchange with identifier PXD032209. The protein interaction network was constructed by the related Gene Ontology (GO) and Kyoto Encyclopedia of Genes and Genomes (KEGG) analysis. Several differentially expressed proteins were validated by Western blot.

Results: Of identified 1598 proteins, 89 were differentially expressed proteins between LPS-A549 cells and Control-A549 cells. Intriguingly, protein-protein interaction network showed that there were 244 significantly enriched co-expression among 60 proteins in the group control-A549. while the group LPS-A549 showed 43 significant enriched interactions among 29 proteins. The related GO and KEGG analysis found evident phenomena of ubiquitination and deubiquitination, as well as the pathways related to autophagy. Among proteins with rich abundance, there were several intriguing ones, including the deubiquitinase (OTUB1), the tight junction protein zonula occludens-1 (ZO-1), the scaffold protein in CUL4B-RING ubiquitin ligase (CRL4B) complexes (CUL4B) and the autophagy-related protein sequestosome-1 (SQSTM1).

Conclusions: In conclusion, our proteomic approach revealed targets related to the occurrence and development of ARDS, being the first study to investigate significant differences in Na, K-ATPase α 1 interacting proteins between LPS-induced ARDS cell model and control-A549 cell. These proteins may help the clinical diagnosis and facilitate the personalized treatment of ARDS.

Keywords: ARDS, Lipopolysaccharide, Proteomics, Na, K-ATPase α 1, A549 cell

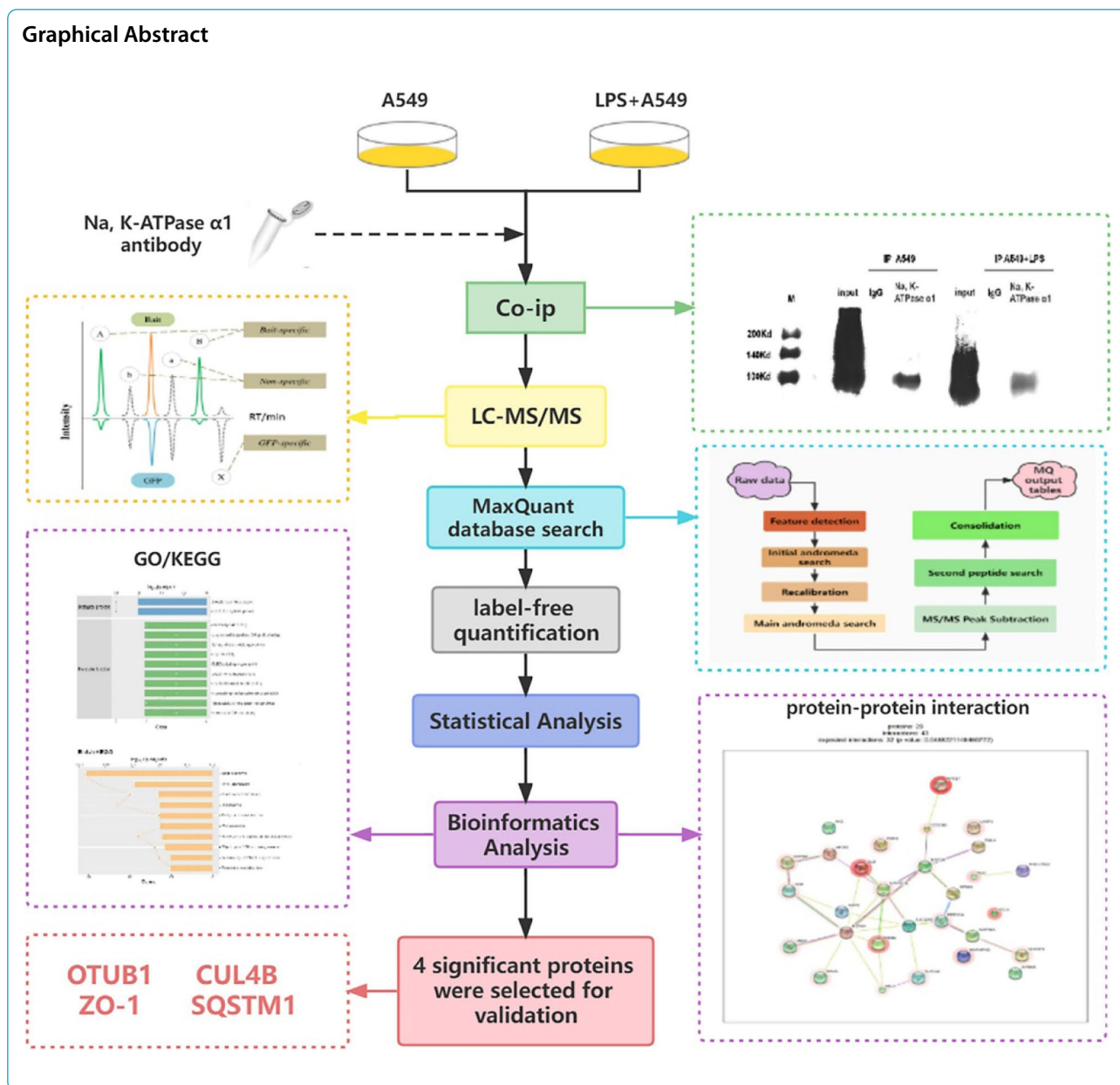
*Correspondence: 13548685542@163.com

¹ Transplantation Center, the Third Xiangya Hospital, Central South University, Changsha 410013, Hunan, China

Full list of author information is available at the end of the article



© The Author(s) 2022. **Open Access** This article is licensed under a Creative Commons Attribution 4.0 International License, which permits use, sharing, adaptation, distribution and reproduction in any medium or format, as long as you give appropriate credit to the original author(s) and the source, provide a link to the Creative Commons licence, and indicate if changes were made. The images or other third party material in this article are included in the article's Creative Commons licence, unless indicated otherwise in a credit line to the material. If material is not included in the article's Creative Commons licence and your intended use is not permitted by statutory regulation or exceeds the permitted use, you will need to obtain permission directly from the copyright holder. To view a copy of this licence, visit <http://creativecommons.org/licenses/by/4.0/>. The Creative Commons Public Domain Dedication waiver (<http://creativecommons.org/publicdomain/zero/1.0/>) applies to the data made available in this article, unless otherwise stated in a credit line to the data.



Introduction

Acute respiratory distress syndrome (ARDS) is a potentially fatal clinical syndrome that occurs as a result of diversified pulmonary and extrapulmonary factors, characterized by excessive lung inflammatory response, impaired tight junction of pulmonary epithelium, decreased pulmonary gas exchange ability and reduced alveolar fluid clearance (AFC) of the lungs with consequent refractory hypoxemia [1]. Effective removal of excess edema fluid in the alveoli and maintenance of dry alveolar space are the main ways to relieve ARDS [2]. The apically-located epithelial Na⁺ channel (ENaC) and

sodium pump, namely Na, K-ATPase, on the basolateral surface of alveolar type II epithelial cells (AT II) mediated sodium ion transport is the main dynamic of AFC [3]. The imbalance of Na, K-ATPase will aggravate the formation of pulmonary edema by limiting Na⁺ transport and destroying the alveolar barrier function [4].

Na, K-ATPase, is a ubiquitous enzyme consisting of three subunits. Among them, α-subunit plays a key role and is the most important one in sodium-water transport as the main driving force of Na⁺ and K⁺ exchange in the lung to promote fluid clearance in the alveoli. There

are four subtypes of α subunit, only $\alpha 1$ exists in lung [5]. Investigating Na, K-ATPase $\alpha 1$ -related pathway may provide new strategies and targets for ARDS treatment. But, a powerful tool to precisely and quantitatively detect changes in protein expression in response to ARDS is necessary.

In the present study, we utilized LPS-induced human AT II cell line (A549) as a model of ARDS [6], and detected the changes in the protein expression profiles of LPS-A549 group compared with control-A549 group and control-IgG group. Currently, the majority of studies on the composition of protein complexes are carried out

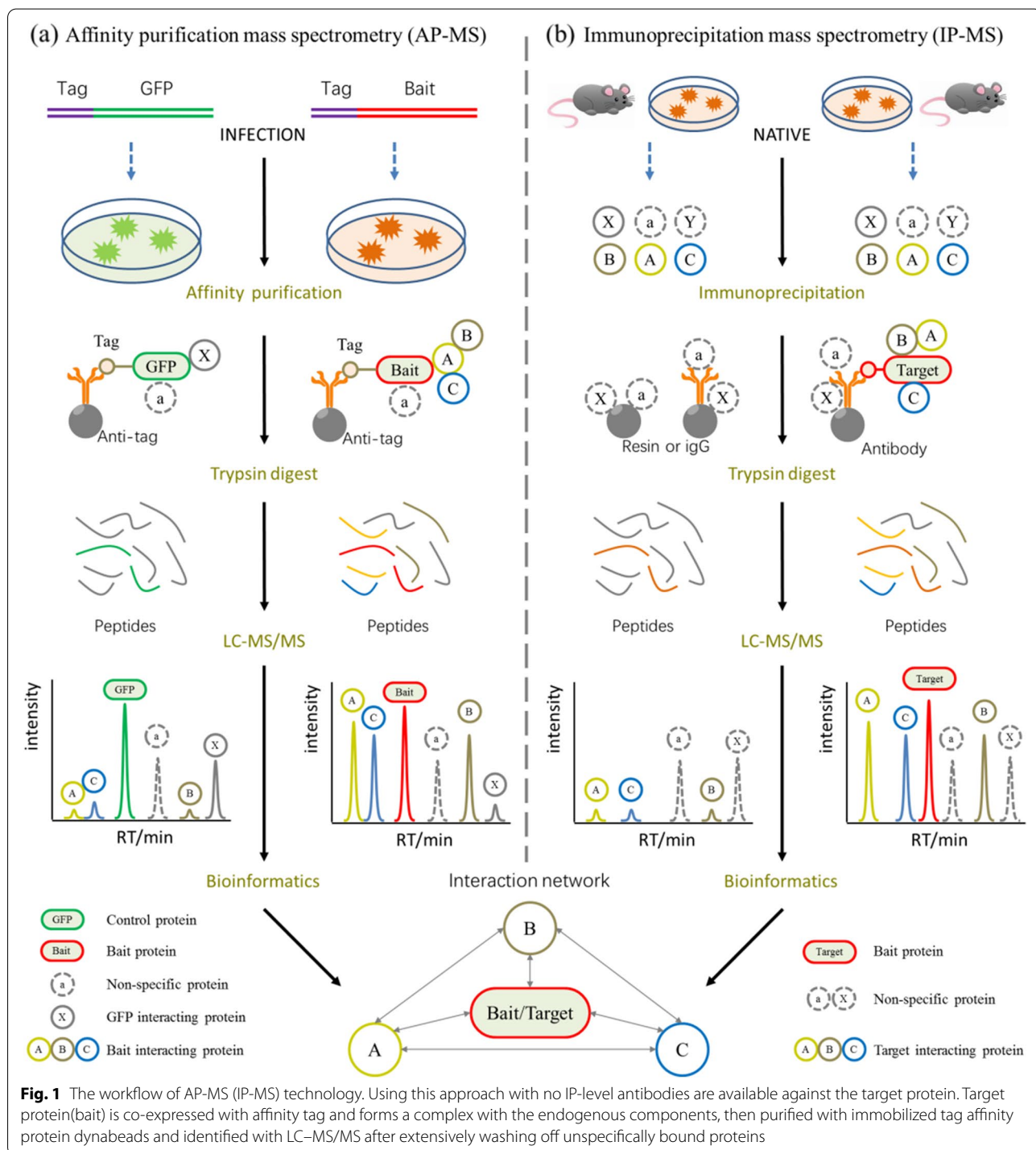
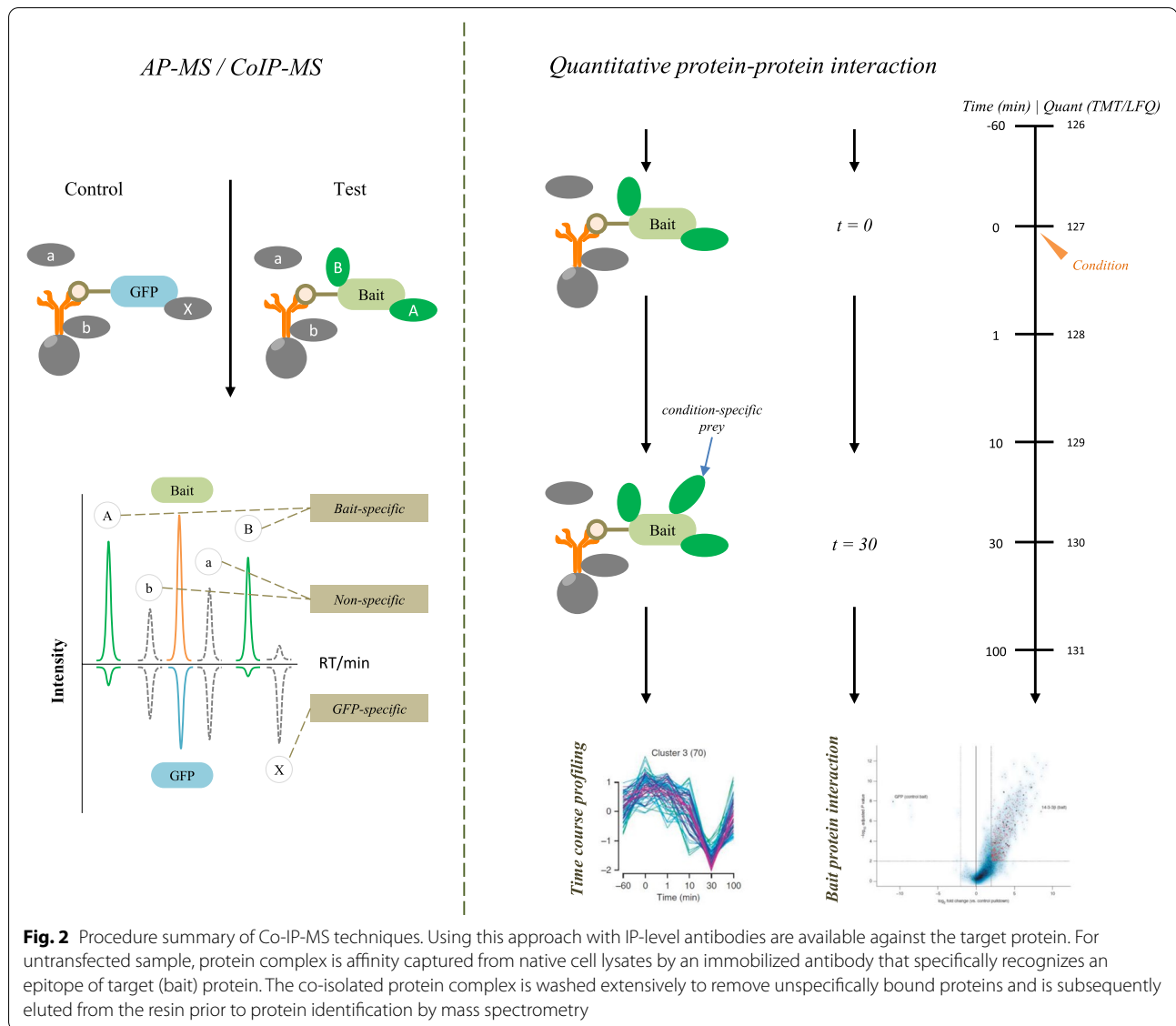


Fig. 1 The workflow of AP-MS (IP-MS) technology. Using this approach with no IP-level antibodies are available against the target protein. Target protein(bait) is co-expressed with affinity tag and forms a complex with the endogenous components, then purified with immobilized tag affinity protein dynabeads and identified with LC-MS/MS after extensively washing off unspecifically bound proteins



by affinity purification mass spectrometry (AP-MS/MS), or by co-immunoprecipitation mass spectrometry (Co-IP-MS) for untransfected native samples, and present a static view of the system (Figs. 1 and 2) (free images were obtained from Aksomics). We employed affinity purification (AP) or co-immunoprecipitation (Co-IP) technology to separate endogenous or labeled bait proteins and the proteins interacting with them. Then, we used liquid chromatography-tandem mass spectrometry (LC-MS/MS) technology to identify and quantify these proteins, combined with Gene Ontology (GO) and Kyoto Encyclopedia of Genes and Genomes (KEGG) analysis, constructing the protein interaction network. Altogether, differential protein expression data may provide a valuable resource to reveal potential molecular targets for ARDS treatment.

Materials and methods

Reagents

LPS (*Escherichia coli* serotype 055: B5) was obtained from Sigma-Aldrich (St Louis, MO, USA); Na, K-ATPase $\alpha 1$ antibody and SQSTM1 rabbit polyclonal antibody were purchased from Proteintech (Chicago, USA); CUL4B rabbit polyclonal antibody was purchased from Immunoway (Newark, DE, USA).

Cell line and cell culture

A549 cell line was purchased from ATCC; A549 cells were seeded into plastic culture dishes at $1 \times 10^6/\text{cm}^2$ and cultured in a humidified incubator (21% O₂, 5% CO₂, 37 °C) in DMEM with 10% fetal bovine serum (FBS), 2 mM L-glutamine, 100 units/ml penicillin, and 100 $\mu\text{g}/\text{ml}$ streptomycin. For all experiments, cells were grown

and maintained in six-well plates, and cells were serum deprived for 24 h prior to pretreatment with LPS at a concentration of 1 µg/ml for 12 h at 37 °C. The final number of cells we used was 2×10^7 A549 cells. This was resuscitated starting from a cryogenic vial, when growing a full T25 culture flask, which was about 1×10^6 cells at that point. Whereas 2×10^7 A549 cells would take 10 flasks, roughly 2–3 weeks.

Sample preparation

There were two groups: A: A549 cells, B: A549 cells + LPS (1 µg/ml, cultured for 12 h). ARDS was induced by LPS according to previous reports [7]. Na, K-ATPase $\alpha 1$ antibody was used to pull down the Na, K-ATPase $\alpha 1$ proteins in two groups of cells. These proteins were pulled down for label-free mass spectrometry to understand the binding and interacting protein, and then the protein of interest was selected for verification.

Co-immunoprecipitation (Co-IP) assay

Fifty microliter anti-igG Dynabeads were used for each sample. Beads were washed 3 times with 500 µL PBSN and shaken gently for 1 min. 2 µg antibody or normal IgG were mixed with 200 µL PBSN. The cleaned Dynabeads were re-suspended and shaken for 1 h at 4 °C slowly. Free antibody was washed out 3 times with 500 µL PBSN and shaken gently for 1 min. Dynabeads were mixed with sample lysate and shaken for 2 h at 4 °C slowly. Then the supernatant was transferred to a new EP tube and stored at -80 °C. Unbinding proteins were washed out with 500 µL PBSN and shaken for 1 min. NP-40, which is incompatible with LC-MS, were washed out with 500 µL PBS4 times. 50 µL 1% TFA was added to Dynabeads and incubated 10 min at 37 °C with highspeed shaking to elute binding proteins. The supernatant was transferred to a new load-binding EP tube. Finally, the elution step was repeated once, combined two elutions, and adjusted to neutral pH with 10% ammonium hydroxide. 100 µL ABC buffer was added for trypsin digest.

LC-MS/MS

LC-MS/MS -based assays were performed as previously described with some minor alterations [8, 9]. For each sample, ~1/2 peptide were separated and analyzed with a nano-UPLC (EASY-nLC1200) coupled to Q-Exactive mass spectrometry (Thermo Finnigan). Separation was performed using a reversed-phase column (100 µm, ID × 15 cm, Reprosil-Pur 120 C18-AQ, 1.9 µm, Dr. Math). Mobile phases were H₂O with 0.1% FA, 2% ACN (phase A) and 80% ACN, 0.1% FA (phase B). Separation of sample was executed with a 120 min gradient at 300 nL/min flow rate. Gradient B: 8 to 30% for 92 min, 30 to 40% for 20 min, 40 to 100% for 2 min, 100% for 2 min, 100

to 2% for 2 min and 2% for 2 min. Data dependent acquisition was performed in profile and positive mode with Orbitrap analyzer at a resolution of 70,000 (@200 m/z) and m/z range of 350–1600 for MS1; For MS2, the resolution was set to 17,500 with a dynamic first mass. The automatic gain control (AGC) target for MS1 was set to 1.0×10^6 with max IT 100 ms, and 5.0×10^4 for MS2 with max IT 200 ms. The top 10 most intense ions were fragmented by HCD with normalized collision energy (NCE) of 27%, and isolation window of 2 m/z. The dynamic exclusion time window was 20 s. The mass spectrometry proteomics data have been deposited to the ProteomeX-change Consortium via the PRIDE [1] partner repository with the dataset identifier PXD032209.

MaxQuant database search

The MaxQuant computational platform was performed as described previously [10]. Raw MS files were processed with MaxQuant (Version 1.5.6.0). The protein sequence database (Uniprot_organism_2016_09) was downloaded from UNIPROT.

Quantification and class specific grouping

We performed proteomic profiling from LPS-A549 cell group and control A549 cell group (Table S1) using the Co-IP and LC-MS/MS technology. In this study, the FDR of polypeptide and protein levels were all controlled at 0.01.

Bioinformatics analysis

Enrichment of gene ontology (GO) terms was measured [11]. Further, pathway analysis for the differentially expressed proteins was carried out by Kyoto Encyclopedia of Genes and Genomes (KEGG) tool which was performed by STRING analysis (<https://string-db.org/>) [12]. The interactions of the proteins were also determined by STRING.

Statistical analysis

All results were expressed as the mean ± standard deviation. The normalized spectral count of protein in purification was performed as previously described [13]. And the difference multiple selection, identification and quantitative results were as follows: FCA value > 1 or FCA value < -1, and the protein with unique peptide number ≥ 2 was defined as significant difference. Statistical significance was set at a $P < 0.05$ (*), $P < 0.01$ (**) and $P < 0.001$ (***)

Results

Na, K-ATPase $\alpha 1$ antibody successfully pulled down the binding proteins of Na, K-ATPase $\alpha 1$ by Co-IP

To verify whether there are proteins that can bind to Na, K-ATPase $\alpha 1$, the total proteins were isolated from cell lysates and then detected by Western blot. A549 cells

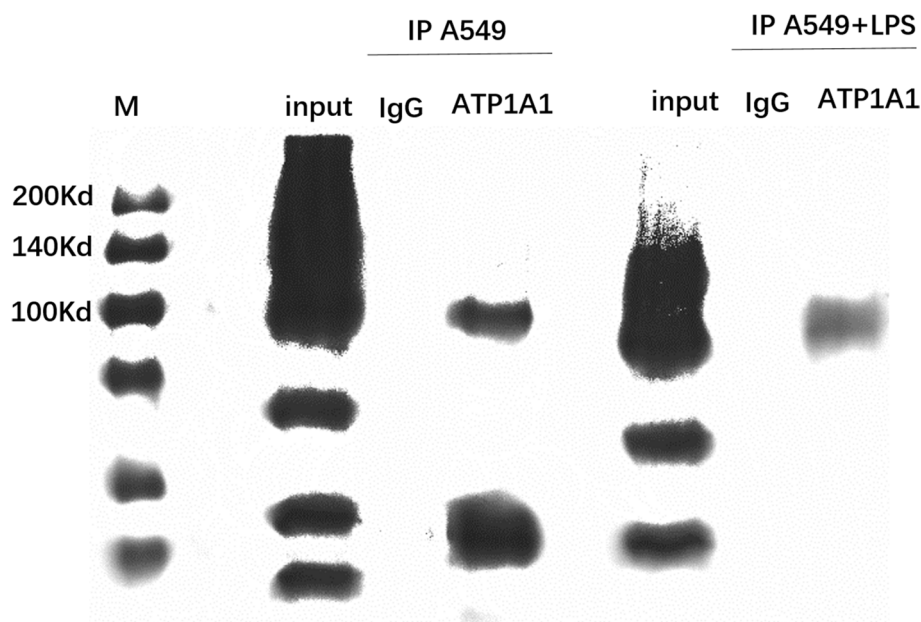


Fig. 3 The binding proteins of Na, K-ATPase $\alpha 1$ in A549 group and A549 + LPS group. The binding proteins of Na, K-ATPase $\alpha 1$ was detected in both groups using Co-IP assay followed by Western blot ($P < 0.001$). Proteins in whole-cell lysate were used as a positive control (input). ATP1A1: the gene name of Na, K-ATPase $\alpha 1$

were divided into two groups: the control-A549 and LPS-A549 groups. The protein expression of Na, K-ATPase $\alpha 1$ was detected in both groups (both $p < 0.001$) (Fig. 3). Thus, we concluded that there were proteins that could interact with and bind to Na, K-ATPase $\alpha 1$ in both groups, from which we could start related proteomic analysis and identify exactly related proteins of Na, K-ATPase $\alpha 1$ in the future work.

Identification and quantification of different proteins

To identify and quantify the significant proteins, in this study, we performed that the total number of identified and quantitated proteins in this assay was 1598, and among them, there are 738 proteins after filtration and 89 differentially expressed proteins in the group LPS-A549 compared with control-A549 (Table S2). Six hundred ninety-eight significant proteins in the group Control-A549 compared with IgG-A549 and 478 significant proteins in the group LPS-A549 compared with IgG-LPS (Table S3).

Respectively, Venn diagrams were then drawn to confirm the different proteins in the three comparisons, namely, LPS-A549 vs. control-A549 (Fig. 4), LPS-A549 vs. IgG-LPS (Fig S1) and control-A549 vs. IgG-A549 (Fig S2). In the discovery phase, we identified that 29 proteins were enriched in the LPS-A549 group, 60 proteins were enriched in the Control-A549 group, and 649 proteins were co-enriched in both groups (Fig. 4). We ranked the

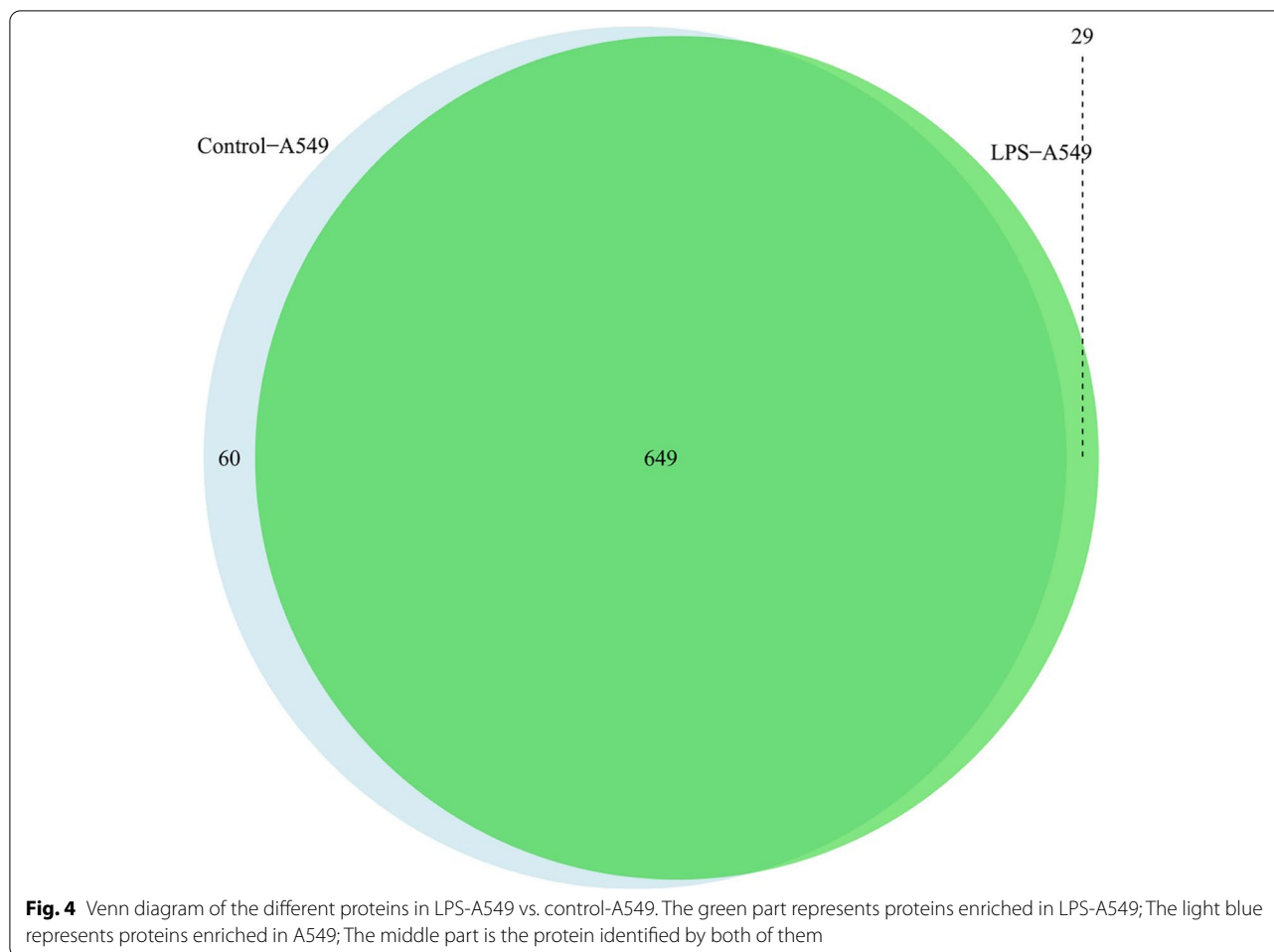
proteins according to fold change in expression levels and listed the top 10 candidates of significantly up-or down-regulated proteins (Table 1). Also, we found that 738 proteins contained E3 ubiquitin ligase or its complex components: TRIP12, RNF21 and CUL4B, deubiquitinases UCHL1, EIF3F and OTUB1, tight junction protein TJP1, and multifunctional protein SQSTM1. Among them, UCHL1 and RNF213 only enriched in the control group, while CUL4B, TRIP12, EIF3F, TJP1, SQSTM1 and OTUB1 enriched in both groups, indicating that they are strongly bound to Na, K-ATPase $\alpha 1$. These analysis results suggested that the difference in proteomic profiling is reliable. In future work, we can select the proteins we are interested in to carry out some relevant verification.

GO & KEGG enrichment analysis of proteins interacting with Na, K-ATPase $\alpha 1$

To search for shared functions among genes, a common way is to incorporate the biological knowledge, by GO and KEGG analysis, to identify predominant biological themes of a collection of genes.

GO enrichment

GO analysis (<http://www.geneontology.org/>) was applied to search for significantly enriched GO terms in areas of biological process (BP), cellular component (CC), and molecular function (MF). Prediction terms with P -value



less than 0.05 were selected and ranked by gene count $((\text{Count}/\text{Pop. Hits})/(\text{List. Total}/\text{Pop. Total}))$ or enrichment score $(\log_{10}(\text{adjust } p\text{-value}))$.

According to the results of group Control-A549 vs. IgG-A549, 750 BP terms, 229 CC terms, and 204 MF terms were found enriched in class-specific test enriched (T) sample compared with control enriched (C) sample. Similarly, in line with the results of group LPS-A549 vs. IgG-LPS, 697 BP terms, 202 CC terms, and 177 MF terms were found enriched in T sample. These generally changed GO terms in T sample and classified by BP, CC, MF, and ranked by gene count and enrichment score (Fig. 5A and B) ($p < 1.0 \times 10^{-7}$ in all terms).

Nevertheless, for what we are concerned about the results of group LPS-A549 vs. Control-A549, only 2 BP terms, 0 CC terms, and 40 MF terms were found enriched in T sample compared with C sample (namely, 1 BP terms, 20 CC terms, and 15 MF terms were found enriched) (Fig. 6A and B). Intriguingly, almost all of the most enriched and meaningful BP terms were related to biosynthetic process in the LPS-A549 group, for instance, “thioester biosynthetic process (GO:0,035,384),”

“acyl-CoA biosynthetic process (GO:0,071,616),” and only “ribosome biogenesis (GO:0,042,254)” in the Control-A549 group. Some more detailed data can be found in (Fig S3 and S4).

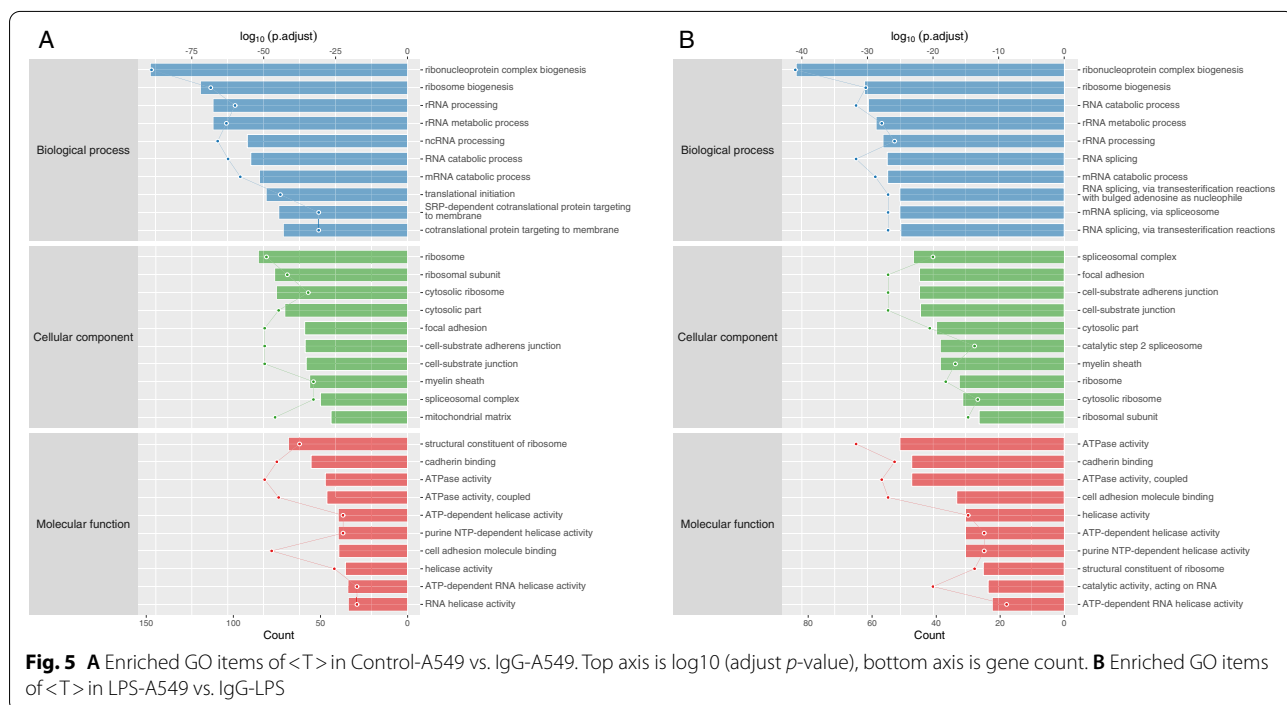
The most enriched CC terms were primarily about the cell in only group control-A549 such as “90S pre-ribosome (GO:0,030,686),” “pre-ribosome (GO:0,030,684),” “melanosome (GO:0,042,470),” “pigment granule (GO:0,048,770),” and “small-subunit processosome (GO:0,032,040).”

As for GO MF terms ranked by either gene count or enrichment score, the mainly enriched terms were closely related to enzymatic activity and protein binding. Represented terms were “misfolded protein binding (GO:0,051,787),” “double-strand/single-strand DNA junction binding (GO:0,000,406),” “formate-tetrahydrofolate ligase activity (GO:0,004,329),” “SUMO activating enzyme activity (GO:0,019,948),” in the LPS-A549 group, and “ATP-dependent RNA helicase activity (GO:0,004,004),” and “ATPase activity (GO:0,016,887).” “ATPase activity, coupled (GO:0,042,623),” in the Control-A549 group.

Table 1 Top 10 up- or down-regulated proteins ranking by FC in LPS-A549 group vs. control-A549 group

Rank	LPS-A549 vs Control-A549		Alias	FC ^a
	Annotation			
Up-regulated Proteins				
1	keratin 17		KRT17	3.20673671
2	dihydrolipoamide dehydrogenase		DLD	2.619500792
3	nicalin		NCLN	2.355100614
4	mutS homolog 2		MSH2	2.355100614
5	heterogeneous nuclear ribonucleoprotein H3 (2H9)		HNRNPH3	1.619500792
6	stearoyl-CoA desaturase (delta-9-desaturase)		SCD	1.619500792
7	LIM and SH3 protein 1		LASP1	1.451281189
8	coatamer protein complex, subunit beta 2 (beta prime)		COPB2	1.451281189
9	coiled-coil domain containing 86		CCDC86	1.355100614
10	solute carrier family 1 (neutral amino acid transporter), member 5		SLC1A5	1.355100614
Down-regulated Proteins				
1	ribosomal RNA processing 1 homolog B		RRP1B	-3.459431619
2	dolichyl-phosphate mannosyltransferase polypeptide 1		DPM1	-2.584962501
3	GDP dissociation inhibitor 2		GDI2	-2.321928095
4	nucleoporin 107 kDa		NUP107	-2.321928095
5	talin 1		TLN1	-2.321928095
6	WD repeat domain 36		WDR36	-2.321928095
7	WD repeat domain 46		WDR46	-2.149102965
8	DEAH (Asp-Glu-Ala-Asp/His) box polypeptide 57		DHX57	-2.000000000
9	G1 to S phase transition 2		GSPT2	-2.000000000
10	nuclear factor of kappa light polypeptide gene enhancer in B-cells 2		NFKB2	-2.000000000

^a FC Fold Change



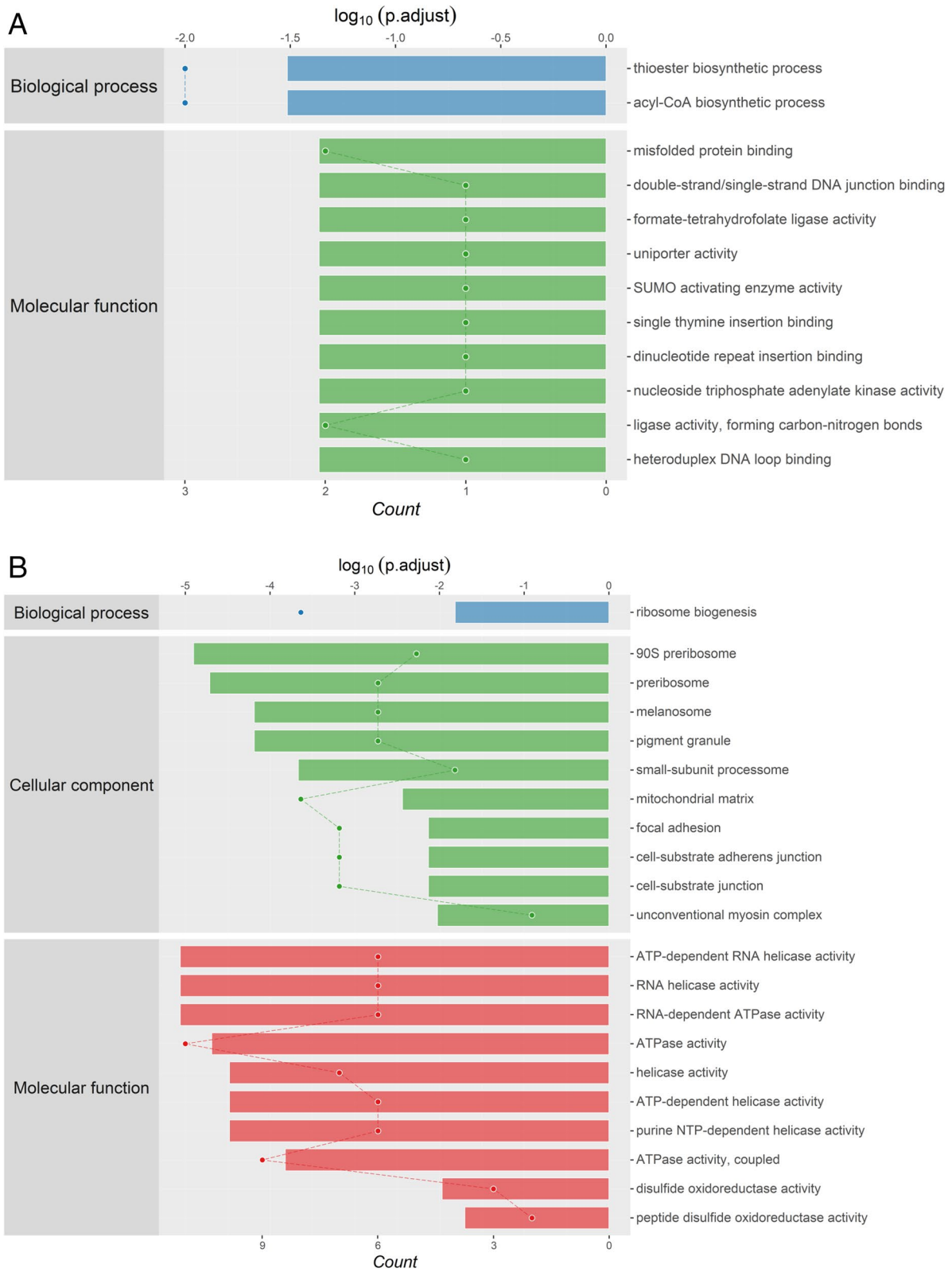


Fig. 6 **A** Enriched GO items of <T> in LPS-A549 vs. Control-A549. **B** Enriched GO items of <C> in LPS-A549 vs. Control-A549

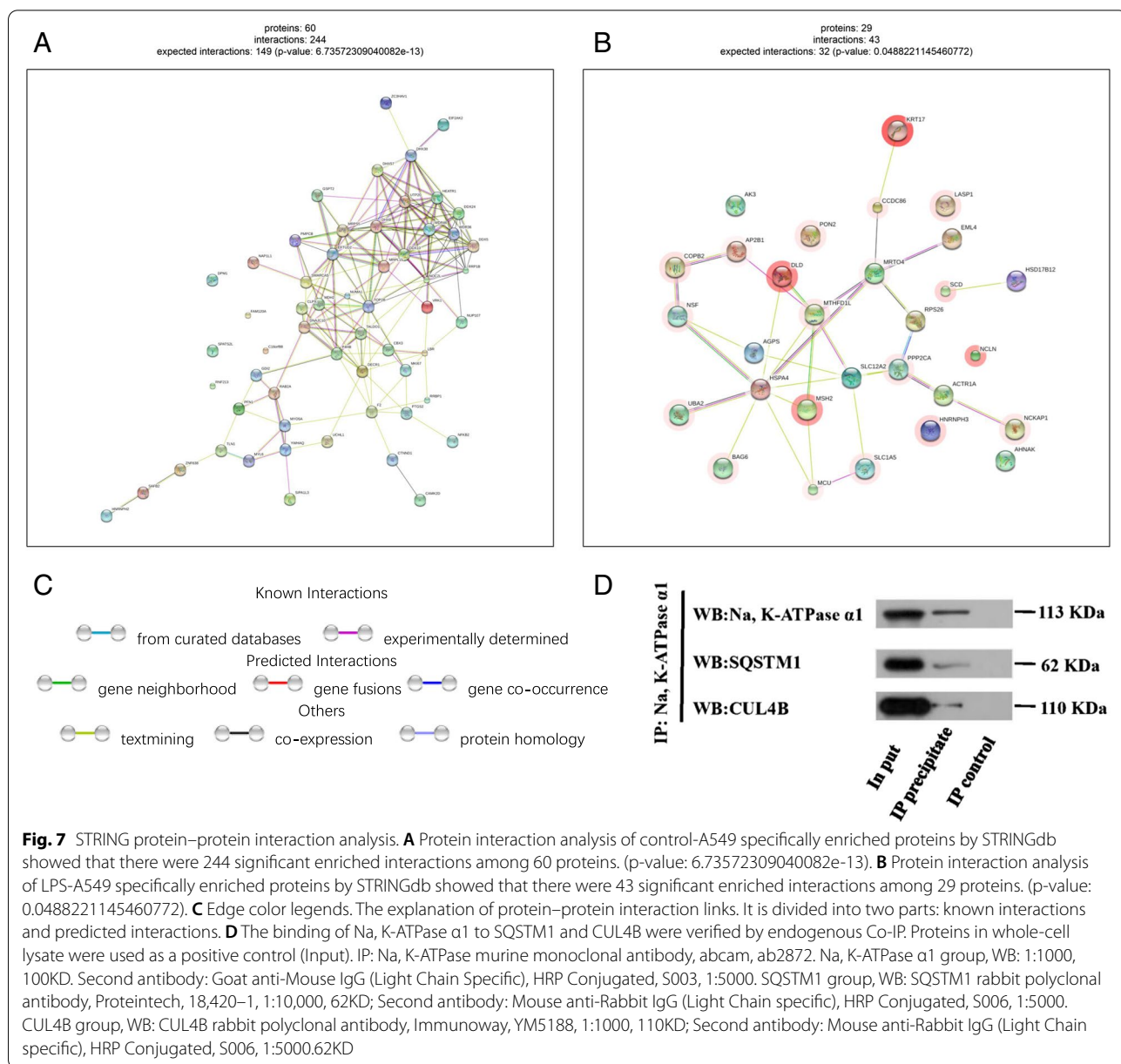
KEGG pathway

We selected differentially expressed proteins for KEGG enrichment analysis, and the results demonstrated that the KEGG pathway was significantly enriched ($p.adjust < 0.05$). Pathways ($p.adjust < 0.05$) were selected and ranked by gene counts. Overall, in the group Control-A549 vs. IgG-A549, 689 differentially expressed proteins were involved in 23 KEGG pathways, like Ribosome, Spliceosome and Carbon metabolism. And in the group LPS-A549 vs. IgG-LPS, 478 differentially expressed proteins were involved in 29 KEGG pathways. The proteins were primarily enriched in RNA transport and Fatty acid metabolism

(Fig S5 and S6). And top 20 pathways were listed for up-regulated genes, respectively (Table S4).

STRINGdb protein–protein interaction (PPI) analysis

To further examine the comprehensive information obtain from the identified protein data, the PPI network was analyzed. The network model was generated using the STRING website. A merged network is shown in (Fig S7 and S8), and, significant proteins annotation (show 50 if available) are shown in (Table S5 and S6). Seven hundred thirty-eight proteins after filter were screened into the PPI network complex, which showed that there were 244 significant enriched interactions among 60 proteins in



the group control-A549 (Fig. 7A). Moreover, in the group LPS-A549, it contained 43 significant enriched interactions among 29 proteins (Fig. 7B). Some explanations of protein–protein interaction links are shown (Fig. 7C).

Ubiquitination and de-ubiquitination enrichment related to OTUB1

In the analysis of protein mass spectrometry, OTUB1 (known as a deubiquitinases) is of particular

interest. OTUB1 belongs to the ovarian cancer proteases family. In this study, we found that Na, K-ATPase α 1 can bind to the deubiquitinase OTUB1 by protein mass spectrometry. Also, in the A549 cell group, GO analysis of Na, K-ATPase α 1 interacting proteins showed significant enrichment of ubiquitination and deubiquitination, both were related to OTUB1. The enrichment items of ubiquitination and deubiquitination enrichment items are shown in (Table 2).

Table 2 The enrichment items of ubiquitination and deubiquitination by GO analysis with Na, K-ATPase α 1 interacting protein

ID	Description	Gene ID
GO: 0016579	Protein deubiquitination	RHOA/SHMT2/PSMC6/PSMA7/PSMD12/PSMC5/PSMC3/PSMA6/PSMC2/RPS27A/PSMC4/UCHL1/PSMD3/EIF3F/PSMD2/ OTUB1 /RUVBL1/PSMA4/PSMD11/PSMA1/PSMB5/VCP/PSMC1/SART3
GO: 0031397	Negative regulation of protein ubiquitination	RPL23/HSPA1A/ OTUB1 /U2AF2/GTPBP4/RPS3/DNAJA1/RPS7/TRIP12
GO: 0031625	Ubiquitin protein ligase binding	RPL23/HSPD1/PA2G4/HSPA1A/RPS27A/EGFR/UCHL1/ OTUB1 /GPI/HSPA9/NDUFS2/YWHAZ/LRPPRC/RTN4/YWHAE/ CUL4B /SLC25A5/TUBB/HSPA5/HSPA8/XRCC5/TCP1/POLR2A/PRDX6/DNAJA1/UQCRC1/VCP/CCT2/ SQSTM1 /FAF2
GO: 0044389	Ubiquitin-like protein ligase binding	RPL23/HSPD1/PA2G4/HSPA1A/RPS27A/EGFR/UCHL1/ OTUB1 /GPI/HSPA9/NDUFS2/YWHAZ/LRPPRC/RTN4/YWHAE/ CUL4B /SLC25A5/TUBB/HSPA5/HSPA8/XRCC5/TCP1/POLR2A/PRDX6/DNAJA1/UQCRC1/STAT1/VCP/CCT2/ SQSTM1 /FAF2
GO: 0070646	Protein modification by small protein removal	RHOA/SHMT2/PSMC6/PSMA7/PSMD12/PSMC5/PSMC3/PSMA6/PSMC2/RPS27A/PSMC4/UCHL1/PSMD3/EIF3F/PSMD2/ OTUB1 /RUVBL1/PSMA4/PSMD11/PSMA1/PSMB5/VCP/PSMC1/SART3
GO: 1903321	Negative regulation of protein modification by small protein conjugation or removal	RPL23/HSPA1A/ OTUB1 /U2AF2/GTPBP4/RPS3/DNAJA1/RPS7/TRIP12
GO: 0033183	Negative regulation of histone ubiquitination	OTUB1 /TRIP12
GO: 1901314	Regulation of histone H2A K63-linked	OTUB1 /TRIP12
GO: 1901315	Negative regulation of histone H2A K63-linked	OTUB1 /TRIP12

Otub1 is marked in red, CUL4B is marked in green, SQSTM1 is marked in blue

Na, K-ATPase α 1 interacts with SQSTM1 and CUL4B through Co-IP and western blot verification

Protein ubiquitination is a key step in the ubiquitin-proteasome degradation pathway, and autophagy plays an indispensable role in maintaining cell homeostasis, clearing excess proteins and organelles, apoptosis, metabolism and senescence. We next selected the autophagy-related protein (SQSTM1) and the scaffold protein in CUL4B-RING ubiquitin ligase (CRL4B) complexes (CUL4B) from the significantly differentially expressed proteins for verification. Western blot assay followed after the Co-IP by Na, K-ATPase α 1 antibody showed that both of SQSTM1 and CUL4B were positive (Fig. 7D), which indicated that there was a close relationship between Na, K-ATPase α 1 and proteins related to autophagy and ubiquitination pathway. In all, further studies are needed to verify these results.

Discussion

Proteomic methods can not only study the whole set of proteins of ARDS, but also verify the drugs that may be effective in the treatment of ARDS. To our knowledge, this study is the first to determine the binding proteins of Na, K-ATPase α 1 in ARDS by proteomic technologies from the perspective of alveolar fluid clearance. Our quantitative discovery-based proteomic approach identified commonalities as well as significant differences in the binding proteins of Na, K-ATPase α 1 between A549 cells and LPS-induced A549 cells. We utilized PPI network analysis to select PPI and gene co-expression proteins that were linked to Na, K-ATPase α 1. Furthermore, we conducted function and pathway analysis to seek biological pathways that may have an impact on ARDS.

We screened these proteins interacted with Na, K-ATPase α 1, and carried out the related GO/KEGG analysis. According to the GO analysis, we found that almost all of the most enriched and meaningful BP terms were related to biosynthetic process in the LPS-A549 group. The mainly enriched terms were closely related to enzymatic activity and protein binding. KEGG analysis showed that the proteins were primarily enriched in RNA transport and Fatty acid metabolism. The PPI network was built on the binding proteins that was analyzed by STRING website. We observed that there were 43 significant enriched interactions among 29 proteins in the LPS-A549 group. Besides, we found that there were obvious ubiquitination and deubiquitination phenomena, as well as the pathways related to autophagy.

Based on these results, we chose some proteins with expression levels that were significantly expressed for further verification. Among the most expressed proteins, there were several intriguing proteins, including the deubiquitinase (OTUB1), the tight junction protein zonula occludens-1 (ZO-1), the scaffold protein

in CUL4B-RING ubiquitin ligase (CRL4B) complexes (CUL4B) and the autophagy-related protein SQSTM1.

Ubiquitination is a type of protein post-translational modification [14]. Our GO analysis of Na, K-ATPase α 1 interaction protein showed that ubiquitination and deubiquitination were significantly enriched, and both were related to OTUB1 (Table 2). OTUB1, known as a deubiquitinase, can protect the protein from degradation and belongs to the ovarian cancer proteases family. Zhang W et al. found that OTUB1 performed as a molecular indicator of poor prognosis in digestive cancers, regulated the infiltration of tumor immunocytes, and exerted a significant influence on apoptosis and autophagy [15]. Our study found that LPS reduced the expression of OTUB1, which may act directly with Na, K-ATPase α 1. Therefore, LPS may decrease the level of Na, K-ATPase α 1 to lessen its protection by decreasing OTUB1. Combined with the previous conclusion, we speculate that up-regulating OTUB1 can protect Na, K-ATPase α 1 from E3 ubiquitin ligase degradation, thus increasing Na, K-ATPase abundance and enzyme activity. More studies are needed to confirm whether OTUB1 can be a therapeutic site for ARDS in the future.

Tight junction is one of the important components of capillary-alveolar barrier, which plays an important role in reducing lung water production and stabilizing lung micro-environment [16]. ZO-1, a tight junction protein, regulates signal transduction, transcription, and cellular communication. The down-regulation of its expression or activity can affect the formation of tight junctions between cells [17, 18]. Ni JJ et al. found that plasma ZO-1 proteins appear to be a valuable prognostic biomarker for the severity of sepsis and a predictor of 30-day mortality for patients with sepsis [19]. And Lee TJ et al. found that ZO-1 on the exotoxin LPS of *P. aeruginosa*-induced diseases could be critical in the development of novel therapeutics [20]. It is interesting that, Na, K-ATPase β 1 promotes the expression of key proteins such as ZO-1, ZO-2, occludin and claudin-18 in tight junction complex and reduces the production of lung water [21]. In our study, the level of ZO-1 mRNA in lung tissue of ARDS rats induced by LPS was significantly lower than that in control group [22]. Accordingly, we speculate that increasing the level of Na, K-ATPase α 1/ β 1 may enhance the tight junction of lung epithelium and reduce the production of lung water. The follow-up experiments are needed to verify our theory.

CUL4B, which acts as a scaffold protein in CUL4B-RING ubiquitin ligase (CRL4B) complexes, participates in a variety of biological processes [23]. Song Y et al. reported that CUL4B functions to restrict TLR-triggered inflammatory responses through regulating the AKT-GSK3 β pathway [24]. Our proteomic results show that CUL4B may bind to Na, K-ATPase α 1 (Fig. 7D), and the therapeutic target site of ARDS may extend to the effect of Na, K-ATPase α 1 on CUL4B in subsequent studies.

SQSTM1 is known as an autophagy protein that is involved in ubiquitin–proteasome and autophagy-lysosome degradation processes [25]. Liu Y et al. revealed that the relationship between Na, K-ATPase and autophagy-lysosome pathway requires the involvement of $\alpha 1$ subunit, and Na, K-ATPase $\alpha 1$ and AMPK may act as the “on” and “off” switch of autophagy pathway [26]. More importantly, Na, K-ATPase can be degraded through the ubiquitin–proteasome pathway and the autophagy-lysosome pathway. Autophagy defects can lead to SQSTM1 accumulation and induce cell stress and disease. In our study, we found that Na, K-ATPase $\alpha 1$ could bind to SQSTM1 by protein profiling, which was verified by endogenous protein interaction analysis (Fig. 7D). Consequently, the decrease of SQSTM1 mRNA expression may be helpful to reduce the transport of polyubiquitinated Na, K-ATPase $\alpha 1$ to autophagy-lysosome system for degradation. The effect of their interaction on the abundance and enzyme activity of Na, K-ATPase $\alpha 1$, the improvement of lung water removal ability of alveolar cells, and the improvement of the prognosis of ARDS is worth extensive attention and discussion in the future.

As we all know, biomarkers are the most direct, rapid and effective diagnostic tools, and their screening and acquisition can play an important role in many aspects of tumor diagnosis, development, treatment, and efficacy monitoring. Consideration these proteins as biomarkers for ARDS have provided valuable insight into the pathogenesis. This is a new hope of identifying new biomarkers for prediction, prognostication, and diagnosis of ARDS. Our study is the first attempt to understand the mechanism of ARDS occurrence by exploring the changes of Na, K-ATPase $\alpha 1$ -binding proteins in ARDS, which can serve to find new targets for drug therapy of ARDS.

Our present study and these previous studies suggest that OTUB1, ZO-1, CUL4B and SQSTM1 can act as therapeutic targets for ARDS cases of different etiologies. For these few proteins we identified, we can develop relevant drugs for targeted therapy. These results are preliminary and require a larger sample size for longitudinal studies and a large number of follow-up animal experiments and clinical trials for validation, which leads to the limitation of our study that the ubiquitin-related, autophagy-related and tight junction related proteins we identified are only present in A549 cells.

Nevertheless, most previous studies have been conducted in lung tissue, plasma, bronchoalveolar lavage fluid of ARDS patients, rats and mice [27], and at the cellular level only Janga H [28] revealed factors associated with LPS-mediated lung injury using H441 epithelial cells and endothelial cells under LS-MS based proteomics. We need to design further studies to investigate whether

these changes are also present in primary mouse alveolar epithelial cells and in lung tissue, plasma and bronchoalveolar lavage fluid in animal models of ARDS. Also, our study might have been more meaningful if we extend these studies to human cell lines, tissues and subjects, as this would provide direct evidence for the role of these proteins in the development of ARDS in human.

Conclusion

In summary, using a quantitative discovery-based proteomic approach, this study identified commonalities as well as significant differences in protein expression profiles of ARDS cells model. Notably, the development of ARDS is related to many pathways. We could roughly screen the important proteins and pathways related to the progression of ARDS, and propose possible therapy of extractive proteins including OTUB1, ZO-1, CUL4B and SQSTM1. These key proteins still need to be tested using a large quantity of clinical specimens, and to be analyzed and validated in combination with the individual conditions of clinical patients. Further well-designed studies developing diagnostic panels and therapeutic targets based on these aberrantly expressed proteins and exploring the roles of these proteins that were most beneficial to ARDS are needed.

Abbreviations

ARDS: Acute respiratory distress syndrome; ALI: Acute lung injury; ICU: Intensive care unit; LC–MS/MS: Liquid chromatography-tandem mass spectrometry; AP–MS/MS: Affinity purification mass spectrometry; Co-IP–MS: Co-immunoprecipitation mass spectrometry; AT II: Alveolar type II epithelial cells; LPS: Lipopolysaccharide; ENaC: Apically-located epithelial Na⁺ channel; A549: Human non-small cell lung cancer cell line/Human AT II cell line; AFC: Alveolar fluid clearance; GO: Gene Ontology; KEGG: Kyoto Encyclopedia of Genes and Genomes.

Supplementary Information

The online version contains supplementary material available at <https://doi.org/10.1186/s12953-022-00193-3>.

Additional file 1: Table S1. Sample grouping. **Table S2.** Experimental results and Statistics. **Table S3.** Summary of significant proteins identified in the study. **Table S4.** Top 20 up-regulated KEGG pathway analysis. **Table S5.** Results of group Control-A549–IgG-A549. Significant proteins annotation (show 50 if available). **Table S6.** Results of group LPS-A549–IgG-LPS. Significant proteins annotation (show 50 if available). **Figure S1.** Venn diagram of the different proteins in LPS-A549 vs. IgG-LPS. **Figure S2.** Venn diagram of the different proteins in control-A549 vs. IgG-A549. **Figure S3.** Enriched GO items of < C > in Control-A549 vs. IgG-A549. top axis is log₁₀(adjust *p*-value), bottom axis is gene count. **Figure S4.** Enriched GO items of < C > in LPS-A549 vs. IgG-LPS. top axis is log₁₀(adjust *p*-value), bottom axis is gene count. **Figure S5.** Enriched KEGG items of < T > in Control-A549 vs. IgG-A549. **Figure S6.** Enriched KEGG items of < T > in LPS-A549 vs. IgG-LPS. **Figure S7.** Control-A549–IgG-A549-STRINGdb-T-1. **Figure S8.** LPS-A549–IgG-LPS-STRINGdb-T-1.

Additional file 2.

Additional file 3.

Additional file 4.

Acknowledgements

We thank KangChen Bio-Tech, Shanghai, China, for their technical support for our experiments;

The mass spectrometry proteomics data have been deposited to the ProteomeXchange Consortium via the PRIDE [1] partner repository with the dataset identifier PXD032209.

Authors' contributions

Design and conduct of the study: QiQuan Wan. Collection of the data: XuPeng Wen, YueZhong Zhang, He Huang, TaoHua Liu. Management, analysis and interpretation of the data: XuPeng Wen and QiQuan Wan. Manuscript preparation: XuPeng Wen. Critical revision: Guo Long, YueZhong Zhang, He Huang and TaoHua Liu. Final approval of the manuscript: All authors.

Funding

This work was supported by the Key project of Hunan Provincial Health Commission, China (grant numbers 202217012851).

Availability of data and materials

The datasets supporting the conclusions of this article are included within the article and its additional files.

Declarations

Ethics approval and consent to participate

Not applicable.

Consent for publication

All the authors have read and approved the manuscript for publication.

Competing interests

All authors declare that there are no conflicts of interest.

Author details

¹Transplantation Center, the Third Xiangya Hospital, Central South University, Changsha 410013, Hunan, China. ²Respiratory ICU, the Third Xiangya Hospital, Central South University, Changsha 410013, Hunan, China. ³Clinical Medicine, Xiangya School of Medicine, Central South University, Changsha 410083, China. ⁴Hunan International Travel Health Care Center, Changsha 410001, Hunan, China.

Received: 4 January 2022 Accepted: 17 May 2022

Published online: 09 June 2022

References

- Griffiths MJD, Mcauley DF, Perkins GD, Barrett N, Blackwood B, Boyle A, Chee N, Connolly B, Dark P, et al. Guidelines on the management of acute respiratory distress syndrome. *BMJ Open Respir Res.* 2019;6(1):e000420.
- Force ADT, Ranieri VM, Rubenfeld GD, Thompson BT, Ferguson ND, Caldwell E, Fan E, Camporota L, Slutsky AS. Acute respiratory distress syndrome: the Berlin definition. *JAMA.* 2012;307(23):2526–33.
- Zhang JL, Zhuo XJ, Lin J, Luo LC, Ying WY, Xie X, Zhang HW, Yang JX, Li D, et al. Maresin1 stimulates alveolar fluid clearance through the alveolar epithelial sodium channel Na_v1, K-ATPase via the ALX/PI3K/Nedd4-2 pathway. *Lab Invest.* 2017;97(5):543–54.
- Laffey JG, Matthay MA. Fifty years of research in ARDS. Cell based therapy for acute respiratory distress syndrome. Biology and potential therapeutic value. *Am J Respir Crit Care Med.* 2017;196(3):266–73.
- Cui X, Xie Z. Protein interaction and Na/K-ATPase-mediated signal transduction. *Molecules.* 2017;22(6):990.
- Rocco PRM, Nieman GF. ARDS: what experimental models have taught us. *Intensive Care Med.* 2016;42(5):806–10.
- Wang Q, Zheng X, Cheng Y, Zhang YL, Wen HX, Tao Z, Li H, Hao Y, Gao Y, et al. Resolvin D1 stimulates alveolar fluid clearance through alveolar epithelial sodium channel, Na_v1, K-ATPase via ALX/cAMP/PI3K pathway in lipopolysaccharide-induced acute lung injury. *J Immunol.* 2014;192(8):3765–77.
- Li J, Zhu HJ. Liquid chromatography-tandem mass spectrometry (LC-MS/MS)-based proteomics of drug-metabolizing enzymes and transporters. *Molecules.* 2020;25(11):2718.
- Wang Z, Wang H, Peng Y, Chen F, Zhao L, Li X, Qin J, Li Q, Wang B, et al. A liquid chromatography-tandem mass spectrometry (LC-MS/MS)-based assay to profile 20 plasma steroids in endocrine disorders. *Clin Chem Lab Med.* 2020;58(9):1477–87.
- Tyanova S, Temu T, Cox J. The MaxQuant computational platform for mass spectrometry-based shotgun proteomics. *Nat Protoc.* 2016;11(12):2301–19.
- Xie C, Li B, Xu Y, Ji D, Chen C. Characterization of the global transcriptome for *Pyropia haitanensis* (Bangiales, Rhodophyta) and development of cSSR markers. *BMC Genomics.* 2013;14:107.
- Liu F, Li W, Li Z, Zhang S, Chen S, Su S. High-abundance mRNAs in *Apis mellifera*: comparison between nurses and foragers. *J Insect Physiol.* 2011;57(2):274–9.
- Morris JH, Knudsen GM, Verschuere E, Johnson JR, Cimermancic P, Greninger AL, Pico AR. Affinity purification-mass spectrometry and network analysis to understand protein-protein interactions. *Nat Protoc.* 2014;9(11):2539–54.
- Wu HQ, Baker D, Ovaa H. Small molecules that target the ubiquitin system. *Biochem Soc Trans.* 2020;48(2):479–97.
- Zhang W, Qiu W. OTUB1 Recruits Tumor Infiltrating Lymphocytes and Is a Prognostic Marker in Digestive Cancers. *Front Mol Biosci.* 2020;7:212.
- Wittekindt OH. Tight junctions in pulmonary epithelia during lung inflammation. *Pflugers Arch.* 2017;469(1):135–47.
- Zhang J, Vincent KP, Peter AK, Klos M, Cheng H, Huang SM, Towne JK, Ferng D, Gu Y, et al. Cardiomyocyte expression of ZO-1 is essential for normal atrioventricular conduction but does not alter ventricular function. *Circ Res.* 2020;127(2):284–97.
- Schwayer C, Shamipour S, Pranjic-Ferscha K, Schauer A, Balda M, Tada M, Matter K, Heisenberg CP. Mechanosensation of tight junctions depends on ZO-1 phase separation and flow. *Cell.* 2019;179(4):937–952e918.
- Ni J, Lu L, Chen H, Xu C, Cai W, Hong G, Zhao G, Lu Z. Plasma ZO-1 proteins predict the severity and outcome of sepsis: a prospective observational study. *Clin Chim Acta.* 2020;510:691–6.
- Lee TJ, Choi YH, Song KS. The PDZ motif peptide of ZO-1 attenuates *Pseudomonas aeruginosa* LPS-induced airway inflammation. *Sci Rep.* 2020;10(1):19644.
- Lin X, Barravecchia M, Kothari P, Young JL, Dean DA. beta-1-Na(+), K(+)-ATPase gene therapy upregulates tight junctions to rescue lipopolysaccharide-induced acute lung injury. *Gene Ther.* 2016;23(6):489–99.
- Wan QQ, Wu D, Ye QF. Candidate genes as biomarkers in lipopolysaccharide-induced acute respiratory distress syndrome based on mRNA expression profile by next-generation RNA-Seq analysis. *Biomed Res Int.* 2018;2018:4384797.
- Liu X, Cui J, Gong L, Tian F, Shen Y, Chen L, Wang Y, Xia Y, Liu L, et al. The CUL4B-miR-372/373-PIK3CA-AKT axis regulates metastasis in bladder cancer. *Oncogene.* 2020;39(17):3588–603.
- Song Y, Li P, Qin L, Xu Z, Jiang B, Ma C, Shao C, Gong Y. CUL4B negatively regulates Toll-like receptor-triggered proinflammatory responses by repressing Pten transcription. *Cell Mol Immunol.* 2021;18(2):339–49.
- Vishnupriya S, PriyaDharshini LC, Sakthivel KM, Rasmi RR. Autophagy markers as mediators of lung injury-implication for therapeutic intervention. *Life Sci.* 2020;260:118308.
- Liu Y, Shoji-Kawata S, Sumpter RM Jr, Wei Y, Ginet V, Zhang L, Posner B, Tran KA, Green DR, et al. Autosis is a Na⁺, K⁺-ATPase-regulated form of cell death triggered by autophagy-inducing peptides, starvation, and hypoxia-ischemia. *Proc Natl Acad Sci U S A.* 2013;110(51):20364–71.
- Wen XP, Zhang YZ, Wan QQ. Non-targeted proteomics of acute respiratory distress syndrome: clinical and research applications. *Proteome Sci.* 2021;19(1):5.
- Janga H, Cassidy L, Wang F, Spengler D, Oestern-Fitschen S, Krause MF, Seekamp A, Tholey A, Fuchs S. Site-specific and endothelial-mediated dysfunction of the alveolar-capillary barrier in response to lipopolysaccharides. *J Cell Mol Med.* 2018;22(2):982–98.

Publisher's Note

Springer Nature remains neutral with regard to jurisdictional claims in published maps and institutional affiliations.